Glutamate 107 in Subunit I of the Cytochrome *bd* Quinol Oxidase from *Escherichia coli* Is Protonated and near the Heme *d*/Heme b_{595} Binuclear Center†

Ke Yang,[‡] Jie Zhang,[‡,§] Ahmet S. Vakkasoglu,[||] Ruth Hielscher,[⊥,#] Jeffrey P. Osborne,[‡,¶] James Hemp,[||] Hideto Miyoshi,[£] Petra Hellwig,[⊥,#] and Robert B. Gennis*[,‡,||]

Department of Biochemistry, and Center for Biophysics and Computational Biology, University of Illinois at Urbana−Champaign, Urbana, Illinois 61801, Institut de Chimie, UMR 7177 LC3, Universite Louis Pasteur, 4, rue Blaise, Pascal, 67000 Strasbourg, France, Institut fuer Biophysik, J. W. Goethe Universitaet, Max von Laue Strasse, 1, 60438 Frankfurt, Germany, Division of Applied Life Sciences, Graduate School of Agriculture, Kyoto University, Sakyo-ko, Kyoto 606-8502, Japan

Received September 19, 2006; Revised Manuscript Received December 22, 2006

ABSTRACT: Cytochrome *bd* is a quinol oxidase from *Escherichia coli*, which is optimally expressed under microaerophilic growth conditions. The enzyme catalyzes the two-electron oxidation of either ubiquinol or menaquinol in the membrane and scavenges O_2 at low concentrations, reducing it to water. Previous work has shown that, although cytochrome *bd* does not pump protons, turnover is coupled to the generation of a proton motive force. The generation of a proton electrochemical gradient results from the release of protons from the oxidation of quinol to the periplasm and the uptake of protons used to form H_2O from the cytoplasm. Because the active site has been shown to be located near the periplasmic side of the membrane, a proton channel must facilitate the delivery of protons from the cytoplasm to the site of water formation. Two conserved glutamic acid residues, E107 and E99, are located in transmembrane helix III in subunit I and have been proposed to form part of this putative proton channel. In the current work, it is shown that mutations in either of these residues results in the loss of quinol oxidase activity and can result in the loss of the two hemes at the active site, hemes *d* and b_{595}. One mutant, E107Q, while being totally inactive, retains the hemes. Fourier transform infrared (FTIR) redox difference spectroscopy has identified absorption bands from the COOH group of E107. The data show that E107 is protonated at pH 7.6 and that it is perturbed by the reduction of the heme *d*/heme b_{595} binuclear center at the active site. In contrast, mutation of an acidic residue known to be at or near the quinol-binding site (E257A) also inactivates the enzyme but has no substantial influence on the FTIR redox difference spectrum. Mutagenesis shows that there are several acidic residues, including E99 and E107 as well as D29 (in CydB), which are important for the assembly or stability of the heme *d*/heme b_{595} active site.

Cytochrome *bd* is a quinol oxidase that is found in many prokaryotes (*1*, *2*). The enzyme is a heterodimer, with the two subunits being encoded by *cyd*A (subunit I, 57 kD) and *cyd*B (subunit II, 43 kD) (*3*). There is no sequence homology between CydA or CydB with the subunits of the heme−copper oxidase superfamily (e.g., cytochrome *c* oxidases) (*4*). Both the heme−copper oxidases and the cytochrome *bd* oxidases are respiratory oxidases and catalyze the four-electron reduction of O_2 to two H_2O. In both types of oxidases, the redox chemistry is coupled to the generation of a proton electrochemical gradient across the membrane (proton motive force). In both groups of oxidases, the sources of electrons and protons that are brought together with O_2 to generate water at the active site are on opposite sides of the membrane. Electrons come from the oxidation of either cytochrome *c* or a quinol, at sites located at the periplasmic side, and protons taken from the cytoplasm. This generates a transmembrane voltage coupled to enzyme turnover. However, whereas the heme−copper oxidases pump protons in addition, the cytochrome *bd* oxidases are not proton pumps.

Both types of oxidases use protons from the bacterial cytoplasm. In the case of the heme−copper oxidases, distinct proton-conducting channels have been structurally and functionally identified (*5*−*10*). The D and K channels are used from proton input, and both lead from the bacterial cytoplasm to the vicinity of the enzyme active site. Highly conserved residues contribute to these channels. It is clear that there must be at least one proton-conducting input channel in the *bd*-type oxidases because the active site of O_2 reduction is located near the periplasmic surface and

† This research was supported by a grant from the National Institutes of Health, HL16101 (to R.B.G.), from the DAAD PPP Program, 04/42419, to P.H., and Grant-in-Aid for Scientific Research from the Japan Society for the Promotion of Science (15380083).

* To whom correspondence should be addressed. Telephone: 217-333-9075. Fax: 217-244-3186. E-mail: r-gennis@uiuc.edu.

‡ Department of Biochemistry, University of Illinois at Urbana−Champaign.

§ Current address: 4664 Cutwater Lane, Hilliard, OH 43026.

|| Center for Biophysics and Computational Biology, University of Illinois at Urbana−Champaign.

⊥ Universite Louis Pasteur.

J. W. Goethe Universitaet.

¶ Current address: Department of Chemistry, Manchester College, North Manchester, IN 46962.

£ Kyoto University.

10.1021/bi061946+ CCC: $37.00
Published on Web 02/17/2007

protons are taken from the cytoplasm to make H_2O (*11*, *12*). Unfortunately, there is no X-ray structure of a *bd*-type oxidase. However, with the large number of sequences now available, one can search for highly conserved residues that might be candidates for such a role. Several years ago, on the basis of sequence alignments, two glutamic acid residues were picked out as prime candidates for being components of a proton-conducting channel, E107 and E99 (*Escherichia coli*) (*12*). These are both predicted to be in transmembrane regions and are conserved. In the current work, the effects of mutations in these as well as other acidic residues are reported.

There are currently about 815 sequences of the cytochrome *bd* genes available from genomic data and environmental sequencing projects. Cytochrome *bd* is much more prevalent in the genomic sequences than in the environmental sequences, which may indicate a biased presence in pathogenic bacteria, which have been a major focus of genomic projects. Indeed, a number of publications have indicated a role of cytochrome *bd* in virulence and the ability of pathogenic bacteria to survive as intracellular parasites (*13*−*17*).

A phylogenetic analysis of the sequences of both CydA and CydB indicates that the *bd*-type oxidase group in four phylogenetically coherent families (Hemp, J., and Gennis, R. B., manuscript in preparation). It has been shown that subunit II has evolved significantly faster than subunit I, leading to more sequence diversity in subunit II (*18*). Many prokaryotes have representatives of more than one of these families, suggesting that they may play distinct roles in the physiology of the organisms. The *E. coli* genome encodes two *bd*-type oxidases (*cyd*AB and *cyx*AB). *Cyx*AB (previously called *app*BC), together with *app*A, consititutes the acid phosphatase regulon (*19*), and the enzyme appears to be optimally expressed under anaerobic or near anaerobic conditions (*20*). The enzyme has not been extensively studied, but it has been isolated and characterized (*21*). The CydAB oxidase has been more extensively studied and is optimally expressed under microaerophilic conditions. CydAB is the predominant oxidase in *E. coli* grown to stationary phase or grown under conditions of limiting O_2 (*22*−*25*). CydAB is part of a closely related subgroup of *bd*-type oxidases that contains an insertion in the C terminus of the Q loop, a large periplasmic "loop" connecting transmembrane helices 6 and 7 (out of 9 predicted transmembrane helices; see Figure 1) (*12*, *26*, *27*). The Q loop has been implicated by many experimental techniques as being involved in ubiquinol binding and oxidation (*28*−*31*).

All of the *bd*-type oxidases contain three hemes. Heme b_{558} is located within CydA, ligated to H186 and M393, and predicted to be near the periplasmic surface (*32*, *33*). The role of heme b_{558} appears to be to facilitate electron transfer from the reduced quinol substrate. The binding of quinone analogues, such as antimycin (*34*) or aurachin D (*29*, *35*), causes a red shift of the absorption spectrum of heme b_{558}. The active site, where O_2 is activated and reduced to water, is composed of two high spin hemes (hemes *d* and b_{595}) that appear to be adjacent and function as a bimetallic center (*36*, *37*). Ferrous heme *d* binds stably to O_2 (heme *d* $Fe^{2+}-O_2$) and, upon the addition of two more electrons, forms a heme *d* $Fe^{4+}{=}O^{2-}$ oxoferryl species (plus ^{-}OH) (*38*). The protein ligand of heme *d* is not known. Heme b_{595} does not stably bind to exogenous ligands (*39*), such as CO, and its role in the catalytic mechanism is not known. It could be present simply as an electron donor, or it could play a role in capturing and activating O_2. Heme b_{595} is ligated to H19 in CydA (*40*), also located at the periplasmic surface (*11*). Hemes *d* and b_{595} are adjacent, and because heme b_{595} is located on the periplasmic surface, it follows that the heme *d*/heme b_{595} active site must be located near the periplasmic side of the membrane (*11*).

Electron transfer from heme b_{558} to the heme *d*/heme b_{595} active site generates a transmembrane voltage (positive outside) (*41*). This cannot be a direct result of the electron transfer itself because heme b_{558} and the heme *d*/heme b_{595} active site are both located near the periplasmic surface. Hence, the voltage must be generated by the coupled movement of protons across the membrane from the cytoplasm to the active site on the opposite side of the membrane. This is the basis for predicting a proton-conducting channel to facilitate this proton translocation.

A number of residues in CydA are totally (>99%) conserved in the 815 sequences (Hemp, J., and Gennis, R. B., manuscript in preparation). These residues include H19 (heme b_{595} ligand) (*40*), H186 and M393 (heme b_{558} ligands) (*32*, *33*), K252 and E257 (implicated in quinone binding) (*29*), R448 (unknown function), and E99, E107, and S140 (suggested as components of a proton channel) (*12*). Slightly less well-conserved (95−99%) are E445 (critical for the electrochemical properties of heme b_{595}) (*41*, *42*), N148 (possible proton-channel component), and R9 (unknown function). Somewhat less conserved (about 85%) are R391 (critical for the electrochemical properties of heme b_{558}) (*43*) and D239 (unknown function), but these are totally conserved within the group of *bd*-type oxidases with a "long Q loop", to which the *E. coli* oxidase belongs. Other conserved residues are glycines, prolines, phenylalanines, or tryptophans, which presumably play structural roles. There is only one totally (>99%) conserved residue (W57) in CydB, which displays much more sequence variation than CydA (*18*). However, acidic residues R100, D29, and D120 are totally conserved within the family of "long Q loop" *bd*-type oxidases, and D58 (*E. coli*) is either an aspartate or glutamate.

In the current work, the results are reported for mutations in several conserved acidic residues: E99, E107, D239, and E257 in CydA and D29 in CydB. The locations in the predicted topology of each subunit are shown in Figure 1. Several mutations result in the loss of hemes *d* and b_{595}: E99A, E99Q, E107D, and D29E (CydB). Mutant oxidases E107Q, D239N, D239A, and E257A have no quinol oxidase activity, but all of the hemes are present in the isolated enzymes.

Fourier transform infrared (FTIR)[1] difference spectroscopy of the wild-type cytochrome *bd* has previously implicated at least one acidic residue as being involved in quinone binding, and more than one acidic residue was shown to be perturbed upon reducing the hemes (*44*, *45*). This approach is extended in the current work. FTIR difference spectroscopy of the E107Q mutant oxidase shows that E107 in the wild-type oxidase is protonated at pH 7.6 and that this residue is

[1] Abbreviations: FTIR, Fourier transform infrared; EDTA, ethylenediaminetetraacetic acid; TMPD, *N*,*N*,*N*′,*N*′-tetramethyl-*p*-phenylenediamine; SHE, standard hydrogen electrode.

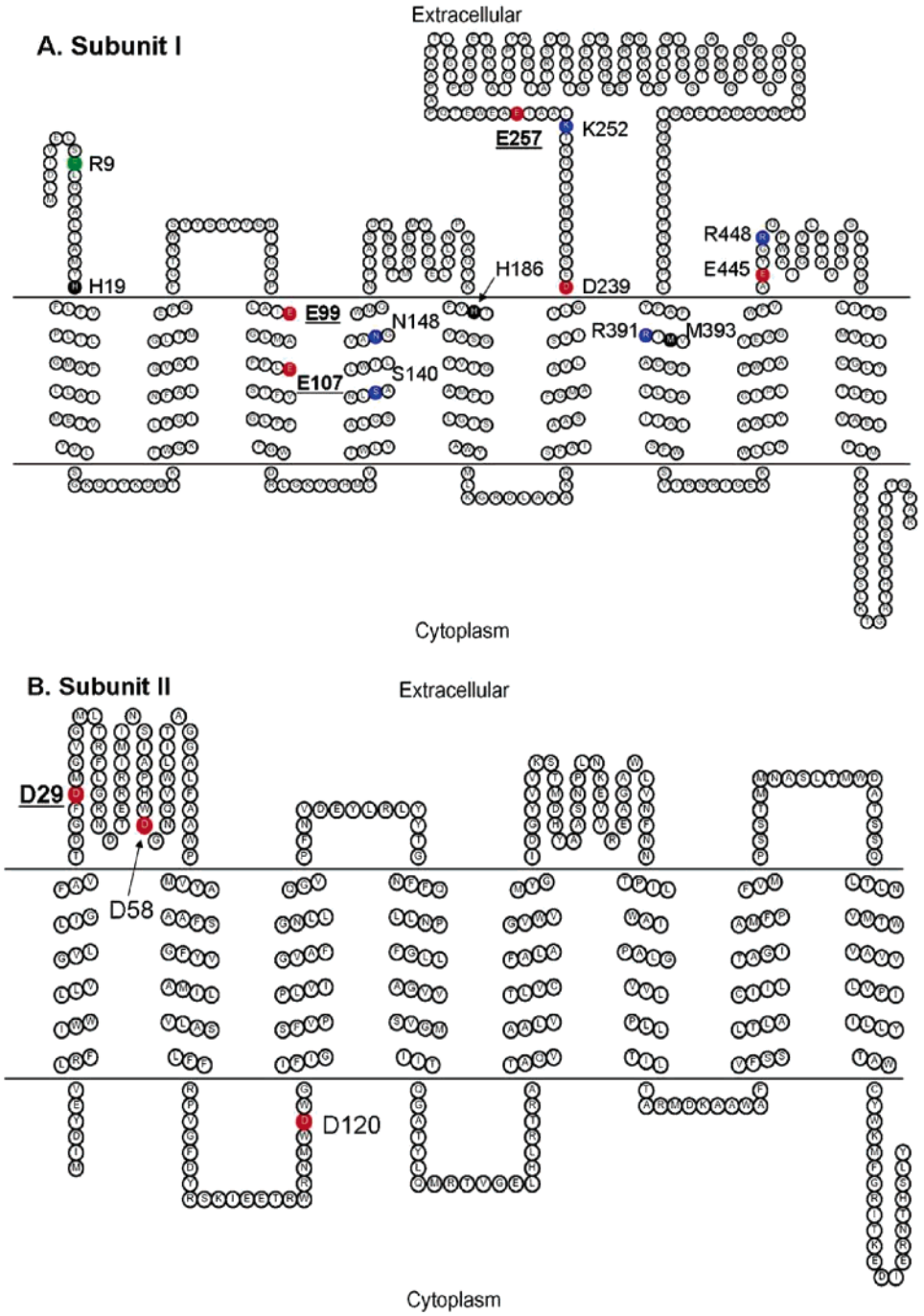

FIGURE 1: Schematic showing the topology of the CydA and CydB subunits of the *bd*-type oxidase from *E. coli*. Conserved residues, which are referred to in the text, are highlighted.

perturbed upon reduction of the heme *d*/heme b_{595} active-site hemes. In contrast, the E257A mutant appears to be located at or near the quinone-binding site, as previously proposed (*29*).

MATERIALS AND METHODS

Strains and Plasmids. *E. coli* strain GO105 (*cyd*AB::*kan*, *cyo*, *recA*), which lacks both cytochrome bo_3 and cytochrome *bd* quinol oxidases (*33*), was used as the host strain for expressing both the wild-type and mutant cytochrome *bd* from a plasmid. To obtain wild-type cytochrome *bd*, plasmid pTK1 (*33*) was introduced into the strain. Mutants of cytochrome *bd* were expressed using pTK1 plasmid as well.

Site-Directed Mutagenesis, Expression, and Complementation Test of the Mutant Cytochrome bd. The Stratagene QuikChange mutagenesis kit was used to construct mutants using plasmid pTK1 (see above) as the template (*42*). The oligonucleotide primers were synthesized by the University of Illinois Biotechnology Center and purified using oligonucleotide purification cartridges with a melting temperature around 80 °C based on the Stratagene formula (*43*). The mutagenesis was performed as described (*42*). All mutations were confirmed by DNA sequencing. The complementation test was carried out as reported previously by Zhang et al. (*42*).

Cell Growth and Protein Sample Preparation. Large-scale cell growth of strains that grow aerobically (i.e., expressing the wild type or E107D mutant) was carried out in 24 2-L flasks, shaking at 220 rpm at 37 °C using an Innova 4330

Table 1: Summary of the Properties of the Cytochrome *bd* Mutants

	complementation of aerobic growth	heme content (UV−vis spectra)[a]	UQ_1H_2 oxidase activity (%)[b]	TMPD oxidase activity (%)[c]
wild type	yes	all hemes present	100	100
E107D	yes	little heme *d* (<15%)	0	0
E107Q	no	low heme *d* content (50%) immediately after preparation; heme *d*/heme b_{595} are labile and readily lost after purification	0	20
E99A	no	no heme *d*/heme b_{595}	0	0
E99Q	no	no heme *d*/heme b_{595}	0	0
E257A	no	wild type	0	50
D239A	no	wild type	0	300
D239N	no	wild type	0	120
D29E (CydB)	no	no heme *d*/heme b_{595}	0	0

[a] Heme *d* values were obtained from the absolute spectrum of the dithionite-reduced enzyme, normalized per milligram of protein, as a very rough estimate. [b] A 100% ubiquinol-1 oxidase activity corresponds to a turnover of about 1450 e^{-1} s^{-1}. The designation "0" means <1% of the wild-type activity. The concentration of cytochrome *bd* in the assay mixture was varied between about 10 and 100 nM. Higher concentrations of enzyme were used to analyze mutants with little or no activity. [c] A 100% TMPD oxidase activity corresponds to a turnover of about 100 e^{-1} s^{-1}. The designation "0" means <1% of the wild-type activity. The concentration of cytochrome *bd* in the assay mixture was varied between about 10 and 100 nM, with higher concentrations used to analyze mutants with little or no activity. The assay is reproducible to within about 10%, and the values presented are rounded off.

incubator shaker (New Brunswick Scientific) (*43*). Strains expressing the wild type and those inactive mutants, which could not grow aerobically, were grown at the Fermentation Facility at the University of Illinois or the OSU Fermentation Facility at 37 °C and pH 7, in a 20-L fermenter using LB containing 100 μg/mL Amp, 50 μg/mL Kan, and 0.3% glucose (*43*).

Both wild-type and mutant cytochrome *bd* oxidases were purified as described previously (*42*). The pooled fractions were concentrated using an Amicon concentrator with a 50 kDa molecular-weight cutoff filter and then dialyzed 3 times against 50 mM sodium phosphate buffer at pH 7.8 containing 5 mM ethylenediaminetetraacetic acid (EDTA) and 0.05% *N*-lauroylsarcosine. Both wild-type and mutant cytochrome *bd* samples were then examined, using the same dialysis buffer for appropriate dilution unless specified otherwise. All of these assays were performed as reported in ref *42*.

UV−Vis Spectroscopic Measurements. All of the absorbance spectra in the UV−vis region and the absorbance spectra for midpoint potential measurements were obtained with a UV-2101PC spectrophotometer (Shimadzu) using a 1-cm path-length cuvette or an ultrathin layer spectroelectrochemical cell (*42*, *43*).

Heme Analysis. The heme *b* contents of both the wild-type and E99Q mutant purified cytochrome *bd* were measured by the pyridine hemochromogen assay, using an extinction coefficient for the wavelength pair 556.5−540 nm = 23.98 mM^{-1} cm^{-1} (*46*). The heme *d* content was determined from the reduced minus "as isolated" difference spectrum, with the $\Delta\epsilon$(628−607 nm) = 10.8 mM^{-1} cm^{-1} (*39*). The concentration of the wild-type cytochrome *bd* was determined from the reduced minus as isolated difference spectrum, using $\Delta\epsilon$(560−580 nm) = 21.4 mM^{-1} cm^{-1} (*47*). Because the "as isolated" enzyme contains varying amounts of the ferrous heme *d*-oxy complex and oxoferryl heme *d* species, the heme *d* content was also determined by the absolute spectrum of the fully reduced enzyme, using the extinction coefficient $\Delta\epsilon_{628-670}$ = 25 mM^{-1} cm^{-1} (*41*).

Ubiquinol-1 and N,N,N′,N′-Tetramethyl-p-phenylenediamine (TMPD) Oxidase Activity Assays. Cytochrome *bd* mutants were assayed in both isolated membranes, in which there is no other quinol oxidase, and with the purified enzyme (*42*). The oxidase activity assays were performed as described previously by Zhang et al. (*42*).

Electrochemistry and FTIR Difference Spectroscopy. FTIR difference spectra recorded at 5 °C as a function of the applied potential with BioRad (now Varian, Inc.) FTS-6000 FTIR. Each FTIR difference spectrum consisted of 256 interferograms at 4 cm^{-1} resolution, and approximately 20 spectra were averaged to give a better signal-to-noise ratio. Triangular apodization is used for Fourier transformation. Equilibration at the applied potential is achieved in less than 10 min. FTIR spectra were monitored until no change was detected. Experimental conditions for *bd* quinol oxidase and electrochemical cell setup are described in detail previously (*42*, *48*). A mixture of 13 different mediators was added to a 40 μM final concentration of 1,1′-dicarboxylferrocene, ferricyanide, dimethylparaphenylendiamine (DMPPD), quinhydrone, tetramethylparaphenylendiamine (TMPPD), tetrachlorobenzoquinone, 2,6-dichlorophenol indophenol, ruthenium hexamine chloride, 1,2-naphthoquinone, menadione, 2-hydroxy-1,4-naphthoquinone, benzyl viologen, and methyl viologen.

RESULTS

The primary motivation of this work was to examine mutations of E107 and E99, which are each totally conserved and predicted to be within a transmembrane span in the CydA subunit (*11*) (Figure 1). In addition, three other highly conserved acidic residues were also replaced by mutagenesis: D239, E257, and D29 (CydB). A summary of the biochemical results are in Table 1 and briefly described below.

(1) E107 was replaced by glutamine and aspartate. The E107Q mutant oxidase was the most useful because it was assembled and the UV−vis spectrum of the isolated enzyme is most similar to that of the wild-type enzyme. The content of heme *d* is about half of that expected compared to the wild type (Table 1), and upon storage, the enzyme loses hemes *d* and b_{595}. There is no ubiquinol oxidase activity, but there is a small amount of TMPD oxidase activity. It has been shown that TMPD donates electrons to a site distinct from ubiquinol and appears to be oxidized directly at the

heme *d*/heme b_{595} active site (*49*). A low activity with TMPD suggests a perturbation of the heme *d*/heme b_{595} active site by the E107Q mutation. Expression of the plasmid-encoded E107Q oxidase in a host strain that has no genomically encoded respiratory oxidases (GO105, *cyd*, *cyo*) does not confer the ability to grow aerobically to the strain. Hence, the E107Q enzyme is isolated from membranes of anaerobically grown cells.

The E107D oxidase does complement GO105, demonstrating that replacing the glutamate by an aspartate results in the assembly of a sufficiently active oxidase to support aerobic growth. However, the isolated E107D mutant oxidase lacks hemes *d* and b_{595} and has no oxidase activity (Table 1). Whole cells from the culture of GO105 expressing E107D do respire, but the respiratory activity is lost upon isolation of the enzyme. Apparently, the mutation destablizes the binding of hemes *d* and b_{595} to a point where even isolation of the membranes results in the loss of activity. These data also support the conclusion that E107 is important for the binding of heme *d*/heme b_{595}.

(2) E99 was replaced by alanine and glutamine. Both the E99A and E99Q mutant oxidases are inactive and do not contain heme *d* or b_{595}. It is concluded that E99, similar to E107, is near heme *d*/heme b_{595} and important for their stable assembly in the protein.

(3) E257 was replaced by alanine. The E257A mutant oxidase lacks ubiquinol oxidase activity but retains significant TMPD oxidase activity (Table 1). Spectroscopically, E257A is similar to the wild-type oxidase, indicating no perturbation of the heme content. Data from the Mogi group (*29*) indicate that E257 is at or near the ubiquinol-binding site, as one might predict based on its location in the Q loop.

(4) D239 was replaced by both asparagine and alanine. Both the D239N and D239A mutant oxidases lack ubiquinol oxidase activity but have TMPD oxidase activity equal to or higher than that of the wild-type oxidase (Table 1). This indicates that the enzyme retains the ability to bind, activate, and reduce O_2 to water. The UV−vis spectra of D239A and D239N are similar to that of the wild type, indicating no perturbation of the heme content. The location of D239 near the Q-loop interface with the membrane (Figure 1) suggests a possible involvement with the ubiquinol-binding site. The midpoint potential of heme *d* was determined for the D239N mutant (data not shown) and compared to that of the wild type. The results show a large decrease in the midpoint potential of heme *d* from the wild-type value of +240 mV [versus standard hydrogen electrode (SHE)] to +100 mV (data not shown).

(5) D29 in CydB was replaced by glutamate. The D29E mutant is totally inactive with either ubiquinol or TMPD as the substrate, and hemes *d* and b_{595} are not present in the isolated enzyme.

One of the goals of this work was to determine whether E107 and/or E99 carboxyl groups contribute to the FTIR redox difference spectrum previously reported (*44*, *45*). Only the E107Q mutant could be isolated with the heme content intact and approximating that of the wild-type oxidase. Figure 2 shows the oxidized-minus-reduced FTIR difference spectra (from +708 to −292 mV versus SHE) of the wild type and E107Q mutant of anaerobically grown cytochrome *bd* oxidase. The spectra include the contributions of all hemes, the bound quinone, the backbone, and all residues reorganizing or changing protonation state concomitant with the redox reaction. The positive signals correspond to the oxidized form, and the negative signals correspond to the reduced state. The spectra of the wild-type oxidase have been previously described in ref *44* and include the contributions of several protonated acidic residues (i.e., COOH). It is noted that anaerobically grown *E. coli* primarily contains menaquinone as a component of its respiratory chain, whereas aerobically grown cells use ubiquinone. Cytochrome *bd* can use either menaquinol or ubiquinol as a substrate. The E107Q mutant enzyme, isolated from anaerobically grown cells, exhibits clear perturbations in the spectral region that is typical for protonated acidic residues (1730−1750 cm^{-1}) (*50*). Other components may also contribute to the FTIR spectrum in this region, including lipids (*51*) and possibly heme *d*, whose FTIR spectrum is unknown. As shown in Figure 2, the FTIR redox difference spectrum of the mutant oxidase differs from that of the wild-type oxidase. The absence of the negative band at 1753 cm^{-1} and the perturbations around 1738 and 1700 cm^{-1} are highlighted in a double-difference spectra in the inset of Figure 2. On the basis of these shifts, E107 can be assigned to the signal in the wild-type spectrum, with a negative trough near 1753 cm^{-1} and positive band at 1738 cm^{-1}. This sigmoid-shaped band is most readily interpreted as being due to the reorganization of the environment around a protonated form of E107. The basic conclusion is that E107 must be protonated at the pH of the experiment (pH 7.6), and it is perturbed upon changing the redox state of one or more of the heme components of the enzyme. The frequencies observed for the residue indicate that E107 is in a hydrophobic environment and that there is stronger hydrogen bonding upon reduction (shift from 1751 to 1738 cm^{-1}).

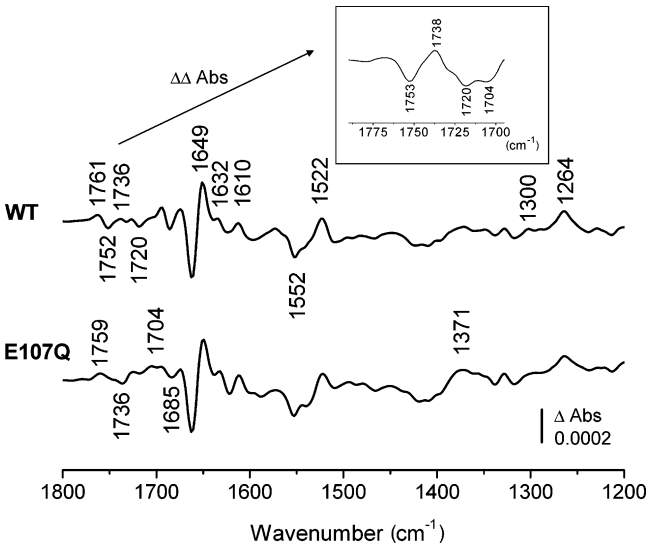

FIGURE 2: Oxidized-minus-reduced FTIR difference spectra of the wild type and E107Q mutant of anaerobically grown cytochrome *bd* for a potential step from +708 to −292 mV versus SHE. The inset shows the enlarged view of a double-difference spectrum obtained by subtracting these spectra.

Additional spectroscopic shifts around 1700 and 1685 cm^{-1} are observed in the spectra, and these spectroscopic changes may include contributions from the heme propionates and the backbone. In the lower spectral range, only minor variations can be seen in the spectrum of the E107Q mutant oxidase, and these may be attributed to the small loss

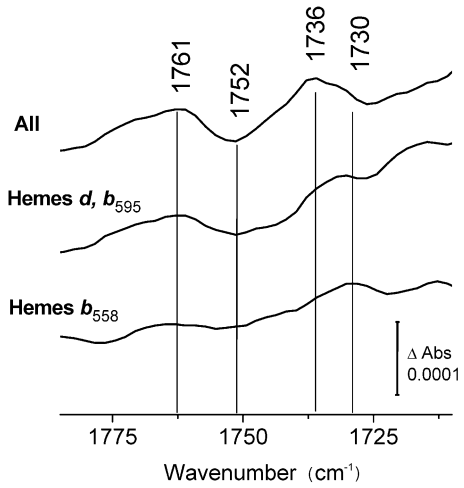

FIGURE 3: Oxidized-minus-reduced FTIR difference spectra of the wild-type cytochrome *bd* for selected potential steps that include the contributions from heme b_{558} (from +118 to −292 mV), the active site (from +708 to +128 mV versus SHE), and a full potential step (from +708 to −292 mV versus SHE), which includes contributions from all cofactors plus the quinone.

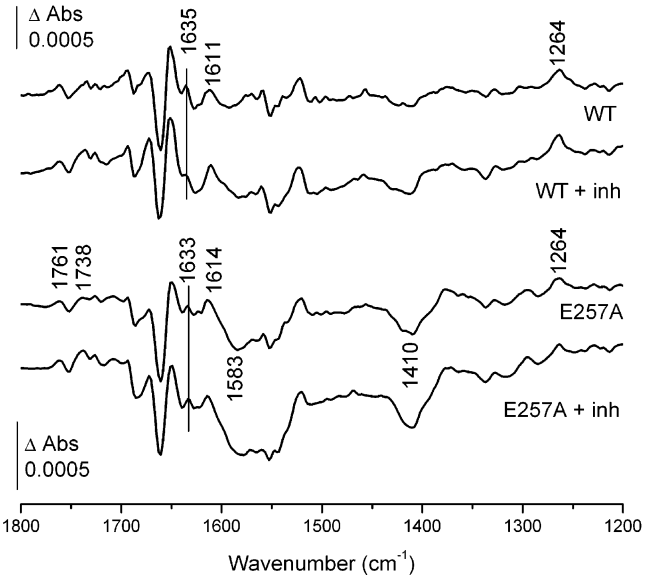

FIGURE 4: Oxidized-minus-reduced FTIR difference spectra of the wild type and E257A mutant of cytochrome *bd* (from +708 to −292 mV versus SHE) with and without the inhibitor aurachin C 1-10. The 1635 cm^{-1} band in the spectrum of the wild-type oxidase is from the bound quinone. This is shifted to 1633 cm^{-1} in the mutant, showing that the quinone remains bound to the E257A mutant oxidase, although there is a perturbation of this C═O mode. In the presence of aurachin C 1-10, the band is significantly reduced in intensity, in the wild-type oxidase, but is not altered in the E257A mutant. Hence, aurachin C 1-10 does not displace the bound quinone. Quinones present in the preparations are a mixture, with menaquinone-8 and ubiquinone-8 being major components. The strong negative features at about 1583 and 1410 cm^{-1} are often observed with mutants of cytochrome *bd*. Although their origin is not known, it seems likely that they are related to the degree to which lipids are present in the preparations.

of heme *d* that is observed over the time required to complete the spectroscopic measurements.

The redox-induced perturbation of the E107 environment was further examined over more narrow ranges of solution potential. Figure 3 shows the double-difference spectrum in the 1750 cm^{-1} region of the spectrum over the ranges from −292 to +118 mV (versus SHE), within which is the midpoint potential of cytochrome b_{558}, and from +128 to +708 mV (versus SHE), which will capture changes accompanying the oxidation/reduction of hemes *d* and b_{595}. The midpoint potentials of hemes *d* and b_{595} are sufficiently close (+256 and +223 mV versus SHE) to preclude resolving spectroscopic changes that can be attributed to either heme alone. The spectral alterations over the entire voltage range (from −292 to +708 mV versus SHE) are also shown in Figure 3, which includes changes coupled to the reduction/oxidation of all three hemes plus the quinones. The results clearly show that the perturbation of the spectrum of E107 is associated with the redox changes of heme *d*/heme b_{595}. There are other changes in the 1750 cm^{-1} region of the spectrum of the wild-type enzyme, suggesting the perturbation of other protonated acidic residues besides E107 coupled to the reduction/oxidation of the metal centers. E99 is a good candidate, but the loss of heme *d*/heme b_{595} from both the E99A and E99Q mutants rules out meaningful FTIR difference spectroscopy.

The E257A mutant was examined by FTIR spectroscopy. The redox difference spectrum, shown in Figure 4, is very similar to that of the anaerobically grown wild-type oxidase in the 1730−1750 cm^{-1} region (*44*). Hence, it is concluded that E257 is not contributing to the redox-coupled spectroscopic changes. Either E257 is not protonated (i.e., not absorbing in the 1750 cm^{-1} region of the spectrum) or, if it is protonated, its environment is not altered by the redox changes.

Previously reported site-directed mutagenesis of E257 has implicated this residue as being at or near the quinol-binding site (*29*). The FTIR redox difference spectrum (Figure 4) shows that the E257A mutant oxidase retains the bound quinone, which is primarily menaquinone. This is demonstrated by the presence of the absorption band at 1633 cm^{-1}, which is assigned to the C═O stretch of a bound quinone (*44*). Another band indicating bound quinone is at 1611 cm^{-1} and present in the E257A mutant spectrum, which is due to the C═C mode (*44*). The 1635 and 1611 cm^{-1} bands are shifted in the E257A mutant spectrum to 1633 and 1614 cm^{-1}, respectively. Both of these shifts may result from a perturbation of the bound quinone. With the wild-type cytochrome *bd*, the 1635 cm^{-1} band is absent when the enzyme is bound to the inhibitor aurachin D (*44*). Presumably, the inhibitor either displaces or alters the binding of the quinone to the protein. The same observation has been made with aurachin C 1-10, which is the *N*-hydroxy derivative of aurachin D and is a somewhat less potent inhibitor of cytochrome *bd* (*35*, *52*). Figure 4 shows the redox difference spectra of the wild-type and E257A mutant oxidase, in the presence and absence of aurachin C 1-10. The 1633 cm^{-1} band is clearly observed in the redox FTIR difference spectrum of the E257A mutant oxidase. This indicates that, under the conditions of this experiment, the quinone (mainly menaquinone) remains bound to the enzyme in the presence of aurachin C 1-10. Under these conditions, the equivalent band in the wild-type oxidase is diminished in magnitude, suggesting partial displacement of the bound quinone. It is concluded that either the binding of aurachin C 1-10 to the E257A mutant oxidase is altered or the effect of the inhibitor binding on the bound quinone is altered by the E257A mutation.

DISCUSSION

Previously reported FTIR difference spectroscopy (*44*, *45*) has shown that more than one acidic residue is perturbed when the metal centers are reduced in cytochrome *bd* from *E. coli*. In addition, at least one acidic residue appears to be protonated at pH 7.6 when the enzyme is bound to menaquinone but deprotonated when the enzyme is bound to ubiquinone (*44*). Three acidic amino acid residues are totally (>99%) conserved in all of the sequences of the *bd*-type oxidases: E99, E107, and E257.

E257. Mutations in E257 (E257A and E257Q) have been examined by Mogi et al. (*29*), and it was concluded that this residue is involved in the binding of the substrate ubiquinol. These mutations each result in about a 3−4-fold increase in the K_m of ubiquinol-1. E257A had a V_{max} that was about 30% of the wild-type value, whereas E257Q had a slightly higher V_{max}. In the current work, the E257A mutant was further examined. Under the conditions of our assay, the E257A mutant is inactive, with ubiquinol-1 as the substrate, and the heme content is normal. The FTIR redox difference spectrum (Figure 4) is similar to that of the wild-type enzyme isolated from anaerobically grown cells. In particular, in the region around 1750 cm^{-1}, the similarity indicates that E257 is not contributing to the spectroscopic perturbations because of the oxidation/reduction of the metal centers. Hence, E257 can be ruled out as the acidic residue whose protonation state is altered depending upon whether ubiquinone or menaquinone is bound to the protein.

In addition, the FTIR redox difference spectrum of the E257A mutant shows that quinone remains bound to the protein. Hence, the loss of function is not due to the elimination of the bound quinone (primarily menaquinone). The data from Mogi et al. (*29*) show that E257 is not essential for the interaction of the enzyme with ubiquinol-1, although mutants do increase the K_m by several fold. In the experiments reported here, the presence of endogenous quinone, mostly menaquinone-8, is reported. The E257A mutant may alter the way in which the quinone binds to the protein and reduce the rate of catalysis. Under our assay conditions (100 μM ubiquinol-1), we have virtually no oxidase activity. Using the values reported for the V_{max} and K_m by Mogi et al. (*29*), we would expect about 5% of the oxidase activity compared to that of the wild type. The reason for the discrepancy, which may be insignificant, will require further investigation.

Figure 4 also shows the FTIR redox difference spectrum of the E257A mutant in the presence of aurachin C 1-10. The 1633 cm^{-1} band is not eliminated by aurachin C 1-10, indicating that either aurachin C 1-10 is not binding under the conditions of the experiment or the binding is perturbed in such a way that the bound quinone is not displaced. With the wild-type oxidase, aurachin C 1-10 under the same conditions results in a spectrum in which the 1633 cm^{-1} band is not present (Figure 4). Mogi et al. (*29*) have shown that the binding of aurachin D to the E257A mutant is not abolished but is perturbed, and the data in Figure 4 are consistent with this result.

E99 and E107. Both the E99A and E99Q mutant oxidases lose the heme *d*/heme b_{595} active site and, therefore, were not useful for FTIR spectroscopy. It is reasonable to conclude that E99 is important for binding the diheme center at the enzyme active site, as is E107. The E107D and E107Q mutants both have labile hemes *d* and b_{595}. In the case of E107Q, the heme content is about half of the expected amount upon isolation, but after 12 h at 4 °C and pH 7.6, the heme *d* content is significantly lower (about half, data not shown). At higher pH, the lability of the hemes is increased, which is the case for the wild-type oxidase as well. The E107D mutant oxidase is functional *in vivo*, but the activity is lost upon preparing membranes and the isolated enzyme lacks hemes *d* and b_{595}. Clearly, E107 is important for both function and the structural integrity of the active site. Evidently, having an acidic residue at this location is not sufficient for stability because aspartate does not substitute for glutamate at this position. This is reflected in the sequence alignments, which show only glutamates at equivalent positions to E99 and E107 (*12*).

The E107Q mutant was sufficiently stable for FTIR difference spectroscopy. The results (Figure 2) show a substantial difference between the spectra of the wild type and E107Q mutant. The double-difference spectrum (inset of Figure 2) clearly shows that E107 absorbs at 1738 cm^{-1} in the oxidized form of the enzyme but at 1752 cm^{-1} when the enzyme is fully reduced. The spectroscopic shift is coupled to the redox change of the heme *d*/heme b_{595} center (Figure 3). The position of the absorption demonstrates that E107 is in a hydrophobic environment and that it is protonated in both the reduced and oxidized forms of the enzyme. Furthermore, the shift to a higher wavenumber indicates that the hydrogen bonding of E107 is strengthened when the enzyme is reduced. Clearly, the population of the enzyme lacking the heme *d*/heme b_{595} active-site hemes does not respond to any redox changes in these metal centers; therefore, these data are not based on the fraction of the enzyme in which these hemes are lacking.

D239 and D29 (CydB). In addition to the three totally conserved acidic residues, the D239A/N and D29E (CydB) mutants were examined. Neither D239 (in subunit I) nor D29 (in subunit II) is totally conserved. However, each of these aspartates is conserved within the family of *bd*-type oxidases with the "long Q loop". D239 is located at the N terminus of the Q loop. Both the D239N and D239A mutant oxidases lack ubiquinol oxidase activity but have high TMPD oxidase activity. The midpoint potential of heme *d* is substantially reduced by the D239N mutation. However, the shift in the midpoint potential is in the opposite direction as would be expected if the influence of D239 on heme *d* was due to the removal of a negative charge from the vicinity of heme *d*. Removing a negative charge by mutagenesis should stabilize the reduced form of the heme, but the opposite is observed. If D239 was deprotonated in the oxidized enzyme but protonated upon reduction, then the D239N mutation might be expected to make it more difficult to reduce heme *d*, as observed. This will require further work to clarify.

D29 in subunit 2 (CydB) is also not totally conserved, but changing this to a glutamate has a dramatic effect on the oxidase: the heme *d*/heme b_{595} center is not present in the isolated enzyme. The N-terminal portion of CydB has been previously implicated in the binding of heme *d*/heme b_{595}. Several randomly selected mutants, which resulted in the loss of heme *d*, were mapped to the N-terminal third of CydB (*53*). Also, proximity mapping, using an artificial protease, demonstrated that residue 39 in CydB is near residue 255 in CydA, which is within the Q loop (*54*).

The data in the current work indicate a cluster of acidic residues from both CydA and CydB that are important for the stable assembly of the heme *d*/heme b_{595} center. These include E99, E107, and D29 (CydB). Even conservative substitutions of glutamate for aspartate or vice versa are not tolerated. The ease of destabilizing the binding of heme *d*/heme b_{595} has been previously noted and speculated to possibly indicate that these hemes are present at the interface between CydA and CydB, susceptible to perturbations at that interface (*53*). The current work is consistent with this possibility but does not rule out other possibilities.

The major motivation of the current work was to investigate the possibility that E99 and E107 participate in conveying protons to the heme *d*/heme b_{595} active site. This remains possible, and the likely proximity of both E99 and E107 to heme *d* is consistent with this role. However, the structural importance of both E107 and E99 make it difficult at this point to make any conclusions about a possible role of these residues in proton translocation within a possible proton channel.

ACKNOWLEDGMENT

We thank Dr. Tatsushi Mogi for assisting in obtaining the aurachin C 1-10, which was used for this study.

REFERENCES

1. Jünemann, S. (1997) Cytochrome *bd* Terminal Oxidase, *Biochim. Biophys. Acta 1321*, 107−127.
2. Mogi, T., Tsubaki, M., Hori, H., Miyoshi, H., Nakamura, H., and Anraku, Y. (1998) Two Terminal Quinol Oxidase Families in *Escherichia coli*: Variations on Molecular Machinery for Dioxygen Reduction, *J. Biochem. Mol. Biol. Biophys. 2*, 79−110.
3. Miller, M. J., Hermodson, M., and Gennis, R. B. (1988) The Active Form of the Cytochrome *d* Terminal Oxidase Complex of *Escherichia coli* Is a Heterodimer Containing One Copy of Each of the Two Subunits, *J. Biol. Chem. 263*, 5235−5240.
4. Pereira, M. M., Santana, M., and Teixeira, M. (2001) A Novel Scenario for the Evoluation of Haem−Copper Oxygen Reductases, *Biochim. Biophys. Acta* 1505, 185−208.
5. Branden, G., Gennis, R. B., and Brzezinski, P. (2007) Transmembrane Proton Translocation by Cytochrome *c* Oxidase, *Biochim. Biophys. Acta*, in press.
6. Brändén, M., Tomson, F. L., Gennis, R. B., and Brzezinski, P. (2002) The Entry Point of the K-Proton-Transfer Pathway in Cytochrome *c* Oxidase, *Biochemistry 41*, 10794−10798.
7. Gennis, R. B. (1998) Multiple Proton-Conducting Pathways in Cytochrome Oxidase and a Proposed Role for the Active-Site Tyrosine, *Biochim. Biophys. Acta 1365*, 241−248.
8. Konstantinov, A. A., Siletsky, S., Mitchell, D., Kaulen, A., and Gennis, R. B. (1997) The Roles of the Two Proton Input Channels in Cytochrome *c* Oxidase from *Rhodobacter sphaeroides* Probed by the Effects of Site-Directed Mutations on Time-Resolved Electrogenic Intraprotein Proton Transfer, *Proc. Natl. Acad. Sci. U.S.A. 94*, 9085−9090.
9. Ostermeier, C., Harrenga, A., Ermler, U., and Michel, H. (1997) Structure at 2.7 Å Resolution of the *Paracoccus denitrificans* Two-Subunit Cytochrome *c* Oxidase Complexed with an Antibody F_v Fragment, *Proc. Natl. Acad. Sci. U.S.A. 94*, 10547−10553.
10. Tsukihara, T., Aoyama, H., Yamashita, E., Takashi, T., Yamaguichi, H., Shinzawa-Itoh, K., Nakashima, R., Yaono, R., and Yoshikawa, S. (1996) The Whole Structure of the 13-Subunit Oxidized Cytochrome *c* Oxidase at 2.8 Å, *Science 272*, 1136−1144.
11. Zhang, J., Barquera, B., and Gennis, R. B. (2004) Gene Fusions with β-Lactamase Show That Subunit I of the Cytochrome *bd* Quinol Oxidase from *E. coli* Has Nine Transmembrane Helices with the O_2 Reactive Site near the Periplasmic Surface, *FEBS Lett. 561*, 58−62.
12. Osborne, J. P., and Gennis, R. B. (1999) Sequence Analysis of Cytochrome *bd* Oxidase Suggests a Revised Topology for Subunit I, *Biochim. Biophys. Acta 1410*, 32−50.
13. Loisel-Meyer, S., Jimenez de Bagues, M. P., Kohler, S., Liautard, J. P., and Jubier-Maurin, V. (2005) Differential Use of the Two High-Oxygen-Affinity Terminal Oxidases of *Brucella suis* for *in Vitro* and Intramacrophagic Multiplication, *Infect. Immun. 73*, 7768−7771.
14. Yamamoto, Y., Poyart, C., Trieu-Cuot, P., Lamberet, G., Gruss, A., and Gaudu, P. (2005) Respiration Metabolism of Group B *Streptococcus* Is Activated by Environmental Haem and Quinone and Contributes to Virulence, *Mol. Microbiol. 56*, 525−534.
15. Shi, L., Sohaskey, C. D., Kana, B. D., Dawes, S., North, R. J., Mizrahi, V., and Gennaro, M. L. (2005) Changes in Energy Metabolism of Mycobacterium Tuberculosis in Mouse Lung and under *in Vitro* Conditions Affecting Aerobic Respiration, *Proc. Natl. Acad. Sci. U.S.A. 102*, 15629−15634.
16. Way, S. S., Sallustio, S., Magliozzo, R. S., and Goldberg, M. B. (1999) Impact of Either Elevated or Decreased Levels of Cytochrome *bd* Expression on *Shigella flexneri* Virulence, *J. Bacteriol. 181*, 1229−1237.
17. Endley, S., McMurray, D., and Ficht, T. A. (2001) Interruption of the *cyd* Locus in *Brucella abortus* Attenuates Intracellular Survival and Virulence in the Mouse Model of Infection, *J. Bacteriol. 183*, 2454−2462.
18. Hao, W., and Golding, G. B. (2006) Asymmetrical Evolution of Cytochrome *bd* Subunits, *J. Mol. Evol. 62*, 132−142.
19. Dassa, J., Fsihi, H., Marck, C., Dion, M., Kieffer-Bontemps, M., and Boquet, P. L. (1991) A New Oxygen-Regulated Operon in *Escherichia coli* Comprises the Genes for a Putative Third Cytochrome Oxidase and for pH 2.5 Acid Phosphatase (*appA*), *Mol. Gen. Genet. 229*, 341−352.
20. Brondsted, L., and Atlung, T. (1996) Effect of Growth Conditions on Expression of the Acid Phosphatase (cyx-appA) Operon and the appY gene, Which Encodes a Transcriptional Activator of *Escherichia coli*, *J. Bacteriol. 178*, 1556−1564.
21. Sturr, M. G., Krulwich, T. A., and Hicks, D. B. (1996) Purification of a Cytochrome *bd* Terminal Oxidase Encoded by the *Escherichia coli app* Locus from a Δ*cyo* Δ*cyd* Strain Complemented by Genes from *Bacillus firmus* OF4, *J. Bacteriol. 176*, 1742−1749.
22. Govantes, F., Orjalo, A. V., and Gunsalus, R. P. (2000) Interplay Between Three Global Regulatory Proteins Mediates Oxygen Regulation of the *Escherichia coli* Cytochrome *d* Oxidase (*cyd*AB) Operon, *Mol. Microbiol. 38*, 1061−1073.
23. Govantes, F., Albrecht, J. A., and Gunsalus, R. P. (2000) Oxygen Regulation of the *Escherichia coli* Cytochrome *d* Oxidase (*cyd*AB) Operon: Roles of Multiple Promoters and the Fnr-1 and Fnr-2 Binding Sites, *Mol. Microbiol. 37*, 1456−1469.
24. Tseng, C. P., Albrecht, J., and Gunsalus, R. P. (1996) Effect of Microaerophilic Cell Growth Conditions on Expression of the Aerobic (*cyo*ABCDE and *cyd*AB) and Anaerobic (*nar*GHJI, *frd*ABCD, and *dms*ABC) Respiratory Pathway Genes in *Escherichia coli*, *J. Bacteriol. 178*, 1094−1098.
25. Iuchi, S., and Lin, E. C. C. (1991) Adaptation of *Escherichia coli* to Respiratory Conditions: Regulation of Gene Expression, *Cell 66*, 5−7.
26. Kusumoto, K., Sakiyama, M., Sakamoto, J., Noguchi, S., and Sone, N. (2000) Menaquinol Oxidase Activity and Primary Structure of Cytochrome *bd* from the Amino-Acid Fermenting Bacterium *Corynebacterium glutamicum*, *Arch. Microbiol. 173*, 390−397.
27. Sakamoto, J., Koga, E., Mizuta, T., Sato, C., Noguchi, S., and Sone, N. (1999) Gene Structure and Quinol Oxidase Activity of a Cytochrome *bd*-Type Oxidase from *Bacillus stearothermophilus*, *Biochim. Biophys. Acta 1411*, 147−158.
28. Matsumoto, Y., Murai, M., Fujita, D., Sakamoto, K., Miyoshi, H., Yoshida, M., and Mogi, T. (2006) Mass Spectrometric Analysis of the Ubiquinol-Binding Site in Cytochrome *bd* from *Escherichia coli*, *J. Biol. Chem. 281*, 1905−1912.
29. Mogi, T., Akimoto, S., Endou, S., Watanabe-Nakayama, T., Mizuochi-Asai, E., and Miyoshi, H. (2006) Probing the Ubiquinol-Binding Site in Cytochrome *bd* by Site-Directed Mutagenesis, *Biochemistry 45*, 7924−7930.
30. Dueweke, T. J., and Gennis, R. B. (1990) Epitopes of Monoclonal Antibodies Which Inhibit Ubiquinol Oxidase Activity of *Escherichia coli* Cytochrome *d* Complex Localize a Functional Domain, *J. Biol. Chem. 265*, 4273−4277.
31. Dueweke, T. J., and Gennis, R. B. (1991) Proteolysis of the Cytochrome *d* Complex with Trypsin and Chymotrypsin Localizes a Quinol Oxidase Domain, *Biochemistry 30*, 3401−3406.
32. Fang, H., Lin, R. J., and Gennis, R. B. (1989) Location of Heme Axial Ligands in the Cytochrome *d* Terminal Oxidase Complex

of *Escherichia coli* Determined by Site-Directed Mutagenesis, *J. Biol. Chem. 264*, 8026−8032.
33. Kaysser, T. M., Ghaim, J. B., Georgiou, C., and Gennis, R. B. (1995) Methionine-393 Is an Axial Ligand of the Heme b_{558} Component of the Cytochrome *bd* Ubiquinol Oxidase from *Escherichia coli*, *Biochemistry 34*, 13491−13501.
34. Jünemann, S., and Wrigglesworth, J. M. (1994) Antimycin Inhibition of the Cytochrome *bd* Complex from *Azotobacter vinelandii* Indicates the Presence of a Branched Electron Transfer Pathway for the Oxidation of Ubiquinol, *FEBS Lett. 345*, 198−202.
35. Meunier, B., Madgwick, S. A., Reil, E., Oettmeier, W., and Rich, P. R. (1995) New Inhibitors of the Quinol Oxidation Sites of Bacterial Cytochromes *bo* and *bd*, *Biochemistry 34*, 1076−1083.
36. Hill, J. J., Alben, J. O., and Gennis, R. B. (1993) Spectroscopic Evidence for a Heme−Heme Binuclear Center in the Cytochrome *bd* Ubiquinol Oxidase from *Escherichia coli*, *Proc. Natl. Acad. Sci. U.S.A. 90*, 5863−5867.
37. Borisov, V. B., Liebl, U., Rappaport, F., Martin, J.-L., Zhang, J., Gennis, R. B., Konstantinov, A. A., and Vos, M. H. (2002) Interactions between Heme *d* and Heme b_{595} in Quinol Oxidase *bd* from *Escherichia coli*: A Photoselection Study Using Femtosecond Spectroscopy, *Biochemistry 41*, 1654−1662.
38. Lorence, R. M., and Gennis, R. B. (1989) Spectroscopic and Quantitative Analysis of the Oxygenated and Peroxy States of the Purified Cutochrome *d* Complex of *Escherichia coli*, *J. Biol. Chem. 264*, 7135−7140.
39. Borisov, V., Arutyunyan, A. M., Osborne, J. P., Gennis, R. B., and Konstantinov, A. A. (1999) Magnetic Circular Dichroism Used To Examine the Interaction of *Escherichia coli* Cytochrome *bd* with Ligands, *Biochemistry 38*, 740−750.
40. Sun, J., Kahlow, M. A., Kaysser, T. M., Osborne, J. P., Hill, J. J., Rohlfs, R. J., Hille, R., Gennis, R. B., and Loehr, T. M. (1996) Resonance Raman Spectroscopic Identification of a Histidine Ligand of b_{595} and the Nature of the Ligation of Chlorin *d* in the Fully Reduced *Escherichia coli* Cytochrome *bd* Oxidase, *Biochemistry 35*, 2403−2412.
41. Belevich, I., Borisov, V. B., Zhang, J., Yang, K., Konstantinov, A. A., Gennis, R. B., and Verkhovsky, M. I. (2005) Time-Resolved Electrometric and Optical Studies on Cytochrome *bd* Suggest a Mechanism of Electron−Proton Coupling in the Di-heme Active Site, *Proc. Natl. Acad. Sci. U.S.A. 102*, 3657−3662.
42. Zhang, J., Hellwig, P., Osborne, J. P., Huang, H.-w., Moënne-Loccoz, P., Konstantinov, A. A., and Gennis, R. B. (2001) Site-Directed Mutation of the Highly Conserved Region near the Q-Loop of the Cytochrome *bd* Quinol Oxidase from *Escherichia coli* Specifically Perturbs Heme, b_{595}, *Bichemistry 40*, 8548−8556.
43. Zhang, J., Hellwig, P., Osborne, J. P., and Gennis, R. B. (2004) Arginine 391 in Subunit I of the Cytochrome *bd* Quinol Oxidase from *Escherichia coli* Stabilizes the Reduced Form of the Hemes and Is Essential for Quinol Oxidase Activity, *J. Biol. Chem. 279*, 53980−53987.
44. Zhang, J., Oettmeier, R., Gennis, R. B., and Hellwig, P. (2002) FTIR Spectroscopic Evidence for the Involvement of an Acidic Residue in Quinone Binding in Cytochrome *bd* from *Escherichia coli*, *Bichemistry 41*, 4612−4617.
45. Yamazaki, Y., Kandori, H., and Mogi, T. (1999) Fourier-Transform Infrared Studies on Conformation Changes in *bd*-Type Ubiquinol Oxidase from *Escherichia coli* upon Photoreduction of the Redox Metal Centers, *J. Biochem. 125*, 1131−1136.
46. Berry, E. A., and Trumpower, B. L. (1987) Simultaneous Determination of Hemes a, b, and c from Pyridine Hemochrome Spectra, *Anal. Biochem. 161*, 1−15.
47. Tsubaki, M., Hori, H., Mogi, T., and Anraku, Y. (1995) Cyanide-Binding Site of *bd*-Type Ubiquinol Oxidase from *Escherichia coli*, *J. Biol. Chem. 270*, 28565−28569.
48. Moss, D., Nabedryk, E., Breton, J., and Mäntele, W. (1990) Redox-Linked Conformational Changes in Proteins Detected by a Combination of Infrared Spectroscopy and Protein Electrochemistry, *Eur. J. Biochem. 187*, 565−572.
49. Lorence, R. M., Carter, K., Gennis, R. B., Matsushita, K., and Kaback, H. R. (1988) Trypsin Proteolysis of the Cytochrome *d* Complex of *Escherichia coli* Selectively Inhibits Ubiquinol Oxidase Activity while Not Affecting *N*,*N*,*N*′,*N*′′-Tetramethyl-*p*-phenylenediamine Oxidase Activity, *J. Biol. Chem. 11*, 5271−5276.
50. Venyaminov, S. Y., and Kalnin, N. N. (1990) in *Biopolymers*, pp 1243−1257, John Wiley and Sons, Inc., New York.
51. Hielscher, R., Wenz, T., Stolpe, S., Hunte, C., Friedrich, T., and Hellwig, P. (2006) Monitoring Redox-Dependent Contribution of Lipids in Fourier Transform Infrared Difference Spectra of Complex I from *Escherichia coli*, *Biopolymers 82*, 291−294.
52. Miyoshi, H., Takegami, K., Sakamoto, K., Mogi, T., and Iwamura, H. (1999) Characterization of the Ubiquinol Oxidation Sites in Cytochromes *bo* and *bd* from *Escherichia coli* Using Aurachin C Analogues, *J. Biochem. 125*, 138−142.
53. Oden, K. L., and Gennis, R. B. (1991) Isolation and Characterization of a New Class of Cytochrome *d* Terminal Oxidase Mutants of *Escherichia coli*, *J. Bacteriol. 173*, 6174−6183.
54. Ghaim, J. B., Greiner, D. P., Meares, C. F., and Gennis, R. B. (1995) Proximity Mapping the Surface of a Membrane Protein Using an Artificial Protease: Demonstration That the Quinone-Binding Domain of Subunit I Is near the N-Terminal Region of Subunit II of Cytochrome *bd*, *Biochemistry 34*, 11311−11315.

BI061946+